Chapter 1

BACKGROUND MATERIAL

1.1 Inside Neutron Stars

The structure and composition of a neutron star depends on its mass and the assumed equation of state of matter at densities above that of the terrestrial nuclear matter. However, all theoretical models of neutron stars predict a liquid interior which contains most of the moment of inertia of the star (the "core") surrounded by a solid metallic crust of neutron rich nuclei and relativistic degenerate electrons. The thin layer (0.5 km) of the outer crust extends over the density range 7×10^6 (g cm^{-3}) $\lesssim \rho \lesssim 4 \times 10^{11}$ (g cm^{-3}) and is surrounded by a surface layer, an atmosphere, only a few meters thick where density falls to zero ; see Fig. 1.1.

In the inner part of the crust at densities $\rho > 4.3 \times 10^{11}$ g cm^{-3} the neutrons begin leaking out of the neutron rich nuclei and form a background fluid of degenerate neutrons surrounding the nuclear lattice. This crustal region extends to densities near the nuclear matter density $\rho_0 \sim 2.4 \times 10^{14}$ g cm^{-3} at which the nuclei dissolve into a dense fluid consisting primarily of neutrons and a small fraction of protons and electrons, all being degenerate. Many other exotic states of matter including neutron solid, and pion condensate have been proposed to exist at densities of a few ρ_0 which will not be of interest to our present study.

Because of the very high thermal conductivity of degenerate matter the temperature

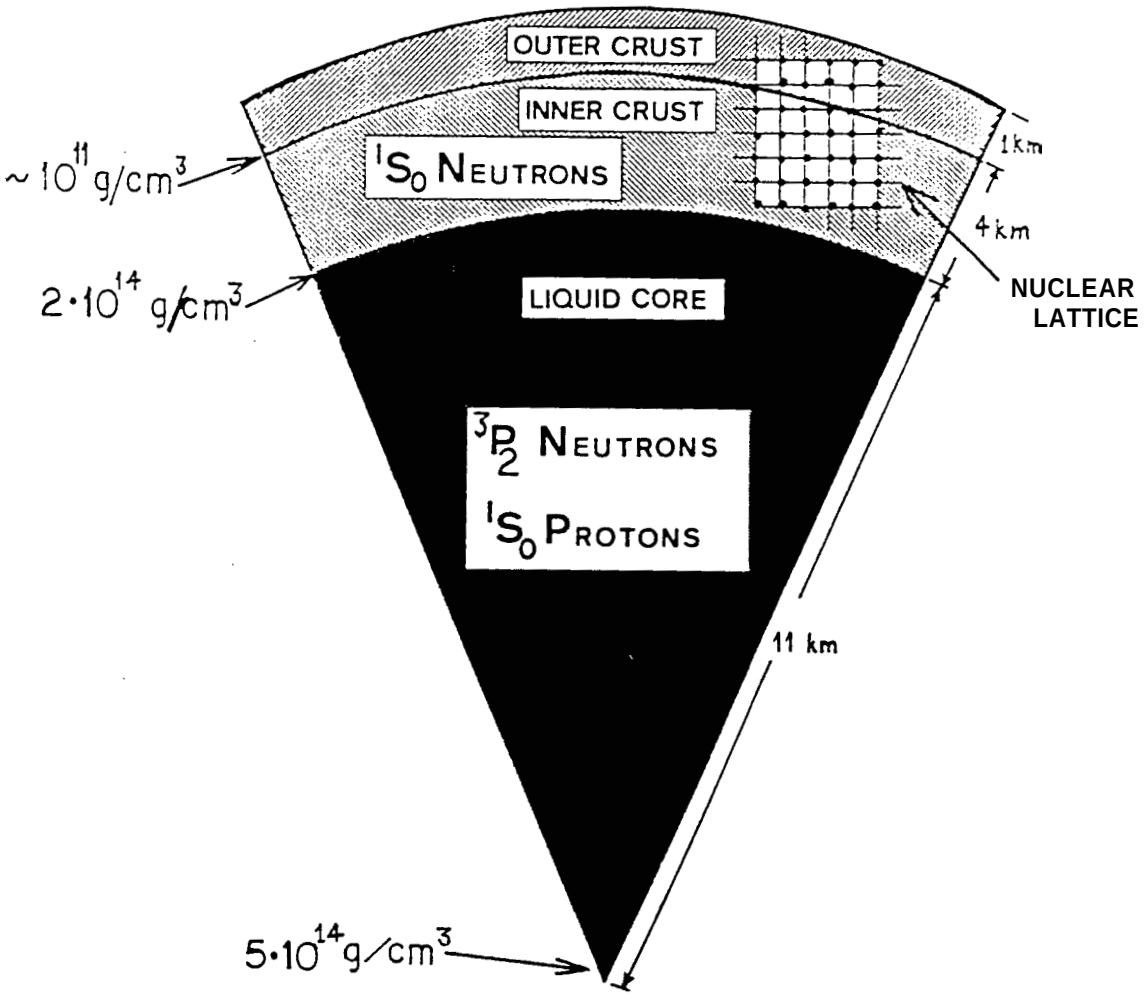

Figure 1.1- Cross section of a 1.4 $M_\odot$ neutron star based on a stiff equation of state. [from Sauls 1989]

T throughout the star is quite uniform and is typically expected to be $\lesssim 5 \times 10^8$ K soon after the formation of the star. Nevertheless the energy gaps and the corresponding critical temperatures for the neutron and proton superfluids are larger than T (see Fig. 1.2). In other words neutron stars are "cold" objects ($T \sim 10^8$ (K) $<< T_{\rm Fermi} \sim 10^{12}$ K). For the same theoretical reasons that terrestrial matter is argued to become superconducting with a transition temperature $T_c \sim 10^{-3}\ T_{\rm Fermi}$ the neutron stars are predicted to have superfluid interiors. In systems of Fermions, as for neutrons and protons in a neutron star, superfluid condensation occurs by the formation of pairs of the Fermions, Cooper pairs, provided there exists an attractive interaction between the particles. However, while for neutrons in the crust and protons in the core the pairs are formed, due to the long-range attractive part of nucleon-nucleon interaction, in an s-wave (internal orbital angular momentum of the pair $|\vec{l}| = 0$) spin-singlet ($|\vec{S}| = 0$, where $\vec{S} = |\vec{s_1} + \vec{s_2}|$ is the total spin of the pair) state, for the neutrons in the density regime of the core of a neutron star spin-triplet ($|\vec{S}| = h$) p-wave ($|\vec{l}| = \hbar$) pairing is favoured because of the higher associated T_c values for the latter, as seen in Fig. 1.2 (Ruderman 1972, Sauls 1989).

In addition to the above theoretical expectation, a strong observational evidence for superfluidity of the interior of neutron stars has been provided by the long time scales of the post-glitch recovery in several pulsars. The observable crust of neutron stars should be coupled to the interior quantum liquid on microscopic time scales were the neutrons and protons "normal" degenerate Fermi liquids. The observed relaxation times of weeks to months imply however that the "strong" interaction scattering between protons and neutrons is quenched, which would be the case if bulk of neutrons (and protons) are in a superfluid state. The coupling of the protons (whether superconducting or not) and electrons in the core to the crust is however believed to be achieved on short time scale ($\sim$ few seconds) through an Ekman pumping process and/or low frequency hydromagnetic waves induced by the stellar magnetic field (Easson 1979; Alpar, Langer & Sauls 1984b). Hence, for the purpose of apalyzing the post-glitch behavior of the star the interior plasma is assumed to be in co-rotation with the solid crust and the magnetic

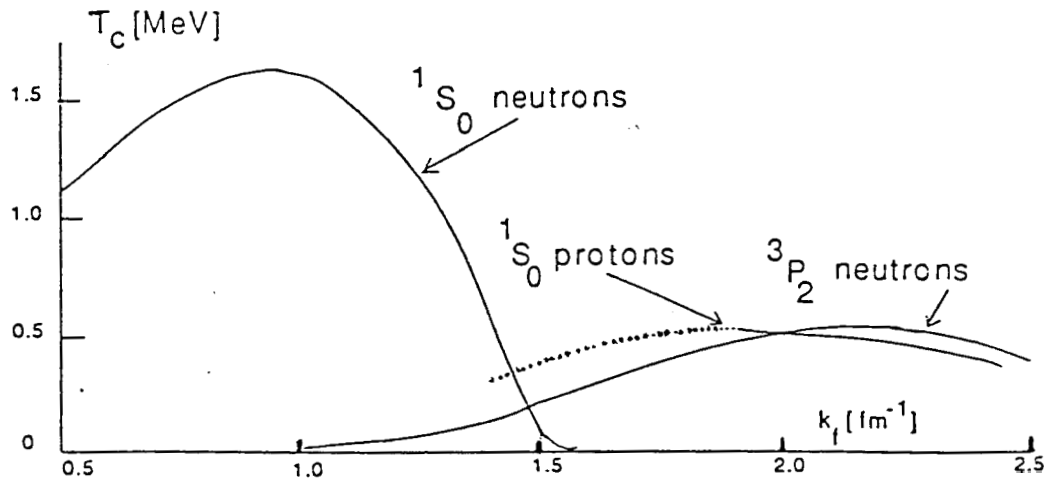

Figure 1.2- Transition teperatures for neutron and proton superfluidity as a function of density expressed in terms of the Fermi wave number $k_f \sim 3 \times n^{\frac{1}{3}}$, where n is the number density in units of fm^{-1}. The cross-over from s-wave pairing to p-wave pairing fro neutrons occurs at approximately 2×10^{14} gcm^{-3}, which is close to the density of the core-crust interface. [from Sauls 1989]

field of the star. The main point of the discussion thus concerns the coupling of the neutron superfluid components in the core and in the crust to the rest of the star which will be referred to as the "crust". On the other hand in order for a superfluid to carry circulation and hence rotate with its vessel (in this case the crust) the condensate must be perforated with vortices, each of a unit circulation κ. The superfluid thus mimics the state of rigid-body rotation along with its vessel through the creation of the required number of vortices (see Fig. 1.3). The problem of dynarnical response of the star to a perturbation, as in a glitch, and the coupling of the superfluid component to the crust therefore reduces to determining the dynamics of vortex motion for the assumed initial conditions (cf. chapter 4).

The existence of superfluid condensates in the interior of a neutron star is expected to profoundly affect the dynarnical, magnetic, and thermal evolution of the star. Furthermore, the dynamical, magnetic, and thermal of a neutron star with neutron superfluid and proton superconductor interior are also believed to be intimately correlated. In the quantum liquid interior of a neutron star a neutron vortex is expected to "pin" to a fluxoid (see Fig. 1.4) should the two structures overlap (Muslimov & Tsygan 1985, Sauls 1989, Srinivasan et al 1990; Jones 1991). The strength of the pinning energy barrier which would impede any relative crossing motion between the fluxoids and the vortices is estimated to be $E_{\rm P} \sim 0.1 - 1.0$ MeV. The mechanism of the pinning is associated with either the proton density perturbations or the magnetized nature of both the vortices as well as the fluxoids (Sauls 1989; Srinivasan et al 1990; Jones 1991).

In addition to the consequences of such pinning effect for the dynamical and the magnetic evolution of neutron stars which are the subject of the present study, the expected frictional motion of superfluid vortices could also be a source of internal heating of the star. The rate of energy dissipation $E_{\rm diss}$ and thus heating of a neutron star due to a superfluid component, with a moment of inertia I_n, which is spinning faster than the crust while maintaining a constant rotational lag w between their angular frequencies during the steady-state slowing down of the star at a rate Ω is given, as for

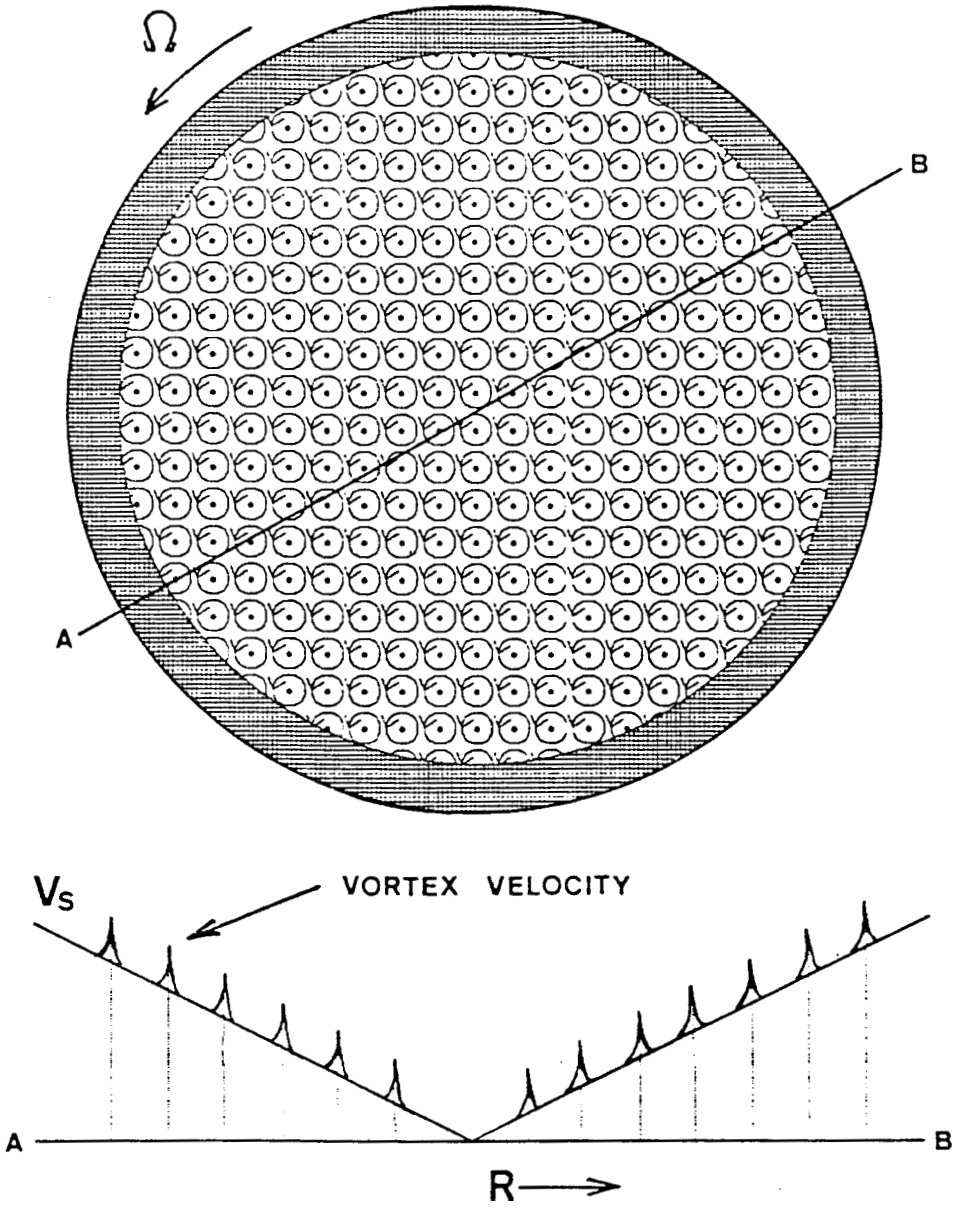

Figure 1.3- Schematic representation of the vortex state of a rotating superfluid at a rate Ω as in the interior of a neutron star is shown at the *top*. The radial dimension of the fluid in the case of the core of the star is R $\sim$ 10 km, the mean distance between vortices is $\sim 10^{-2}$ cm for a young pulsar, and the radial dimension of a vortex core is $\sim$ 100 fm. The *bottom* part of the figure shows the profile of the superfluid velocity along a line through the center of rotation (line A–B). The rotational velocity of the superfluid deviates from the rigid-body value of $R\Omega$ only near the central parts of the vortices, where the individual vortex velocity field ($\propto$ inverse of the distance from the center of that vortex) dominates the average velocity induced by all other vortices. [from Sauls 19891

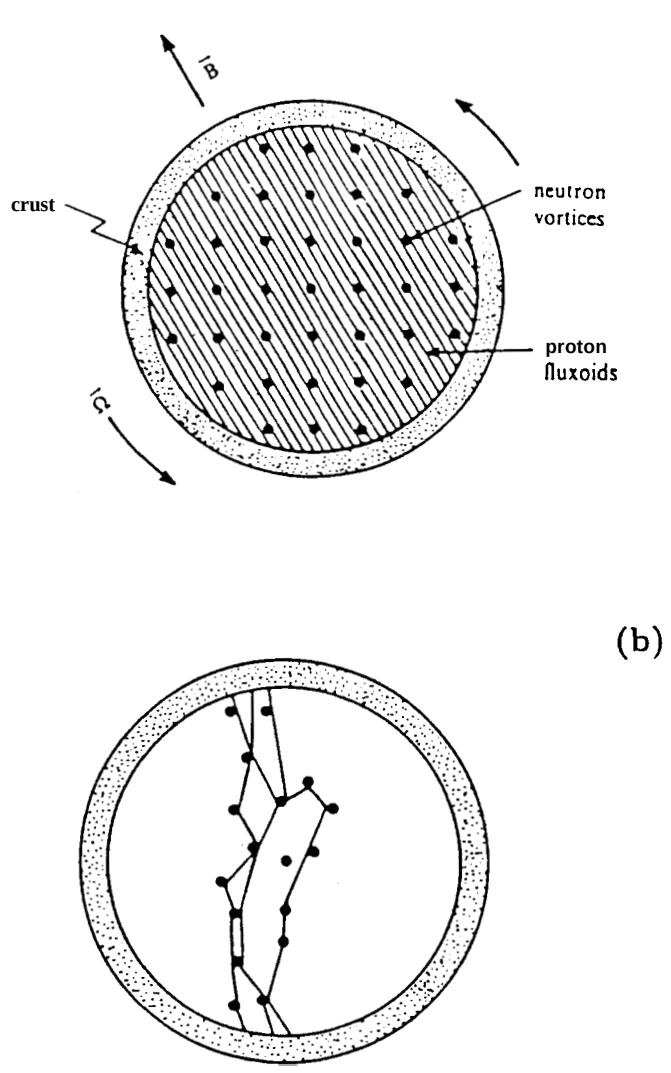

Figure 1.4- *a)* A view of the equatorial plane of the core of a rotating neutron star showing an idealized geometry of the arrangement of the neutron superfluid vortices (parallel to the rotation axis) and the proton superconductor fluxoids (parallel to the magnetic axis). For the purpose of illustration the magnetic axis has been assumed to be perpendicular to the rotation axis. b) A more realistic state of affairs in the presence of strong interaction between the vortices in the two superfluid mixture. [from Srinivasan et al. 1990]

any two dynamically coupled systems with relative velocities between them, by

$$E_{\rm diss} = I_{\rm p}\,\omega\,\dot{\Omega} \tag{1.1}$$

The effect of a superfluid component in the crust of neutron stars on the thermal evolution of the star have been already discussed (Pines & Alpar 1985; Shibazaki & Lamb 1989; Link & Epstein 1996) which might be generalized to the case of core superfluid. The corresponding rate of heating $E_{\rm diss}$ due to the core superfluid might be however expected to be of the same order of magnitude as that of the crust superfluid component. This is because the larger value of $I_{\rm p}$ in the case of core superfluid is compensated by its smaller steady-state lag than that invoked for the crust.

1.2 Recycling of Pulsars

Young radio pulsars, neutron stars in binary X-ray sources, and old binary (and/or millisecond) radio pulsars are considered to represent three successive stages of the evolution of a neutron star in a binary, according to the recycling scenario (Radhakrishnan & Srinivasan 1984). The binary and millisecond pulsars as a group differ from the bulk of normal single pulsars by having on average much faster spins and much weaker surface magnetic fields. As can be seen from Fig. 1.5, most binary pulsars and all of the millisecond pulsars fall outside the pulsar "island" on the $B_{\rm s}$–$P_{\rm s}$ diagram. While less than 2% of all pulsars in the galactic disk are found in binaries, however some 50% of the millisecond pulsars are found in binaries (van den Heuvel 1994). Or put it another way, more than half of the known binary pulsars (and all millisecond pulsars) have $P_{\rm s} < 12$ ms whereas 97% of all pulsars have $P_{\rm s} \gtrsim 30$ ms (Bhattacharya & van den Heuvel 1991).

The binary radio pulsars are furthermore divided into two classes, according to their orbital characteristics and the estimated masses of their companions. The two classes of binary radio pulsars are in fact associated with the final evolutionary products of the two classes of binary X-ray sources which are thought to be neutron stars accreting matter from their unevolved companion stars. Evolution of the X-ray sources consisting

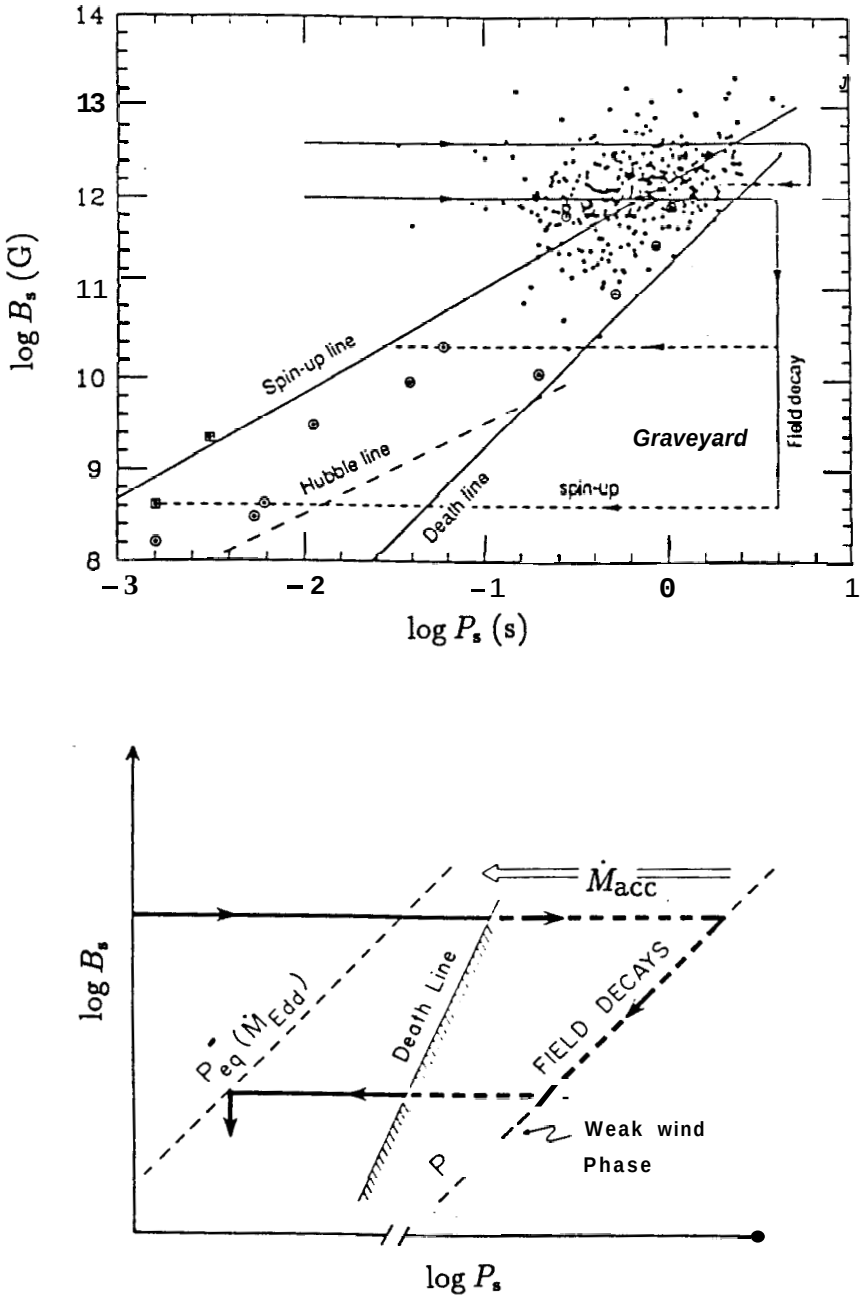

Figure 1.5- The B_s–P_s diagram for the observed single *(dots)* and binary *(circles)* pulsars. Possible evolutionary tracks of pulsars recycled in binaries are indicated. Pulsars are born in the left upper part of the diagram and, if no field decay occurs, move towards the right along horizontal tracks *(full lines).* In the graveyard, assuming the field to decay, they move downward. Accretion causes the spin-up and the leftward movement of pulsars in the diagram as is shown by *dashed lines.* The *bottom* diagram shows alternative evolutionary routes depending on the strength of the magnetic field and the accretion rate. The equilibrium period line corresponding to the Eddington accretion rate is shown at the extreme left. [from van den Heuvel 1994, and Srinivasan 1989]

a neutron star and a high-mass mainsequence companion (HMXBs) is predicted to result in relatively narrow orbits due to occurrence of a spiral-in phase. This happens when the companion evolves off the mainsequence and transfers mass at a very large rate which cannot be accreted promptly. Thus it surrounds the whole system, forming a so-called "common-envelope" that causes a frictional motion at the cost of the orbital energy and hence the orbit shrinks. The fate of the companion of the neutron star in these systems is to become either another neutron star in an eccentric orbit or a massive C-O white dwarfs in a circular orbit. On the other hand, pulsars recycled in the other class of X-ray binaries having low-mass companion stars (LMXBs) are predicted to be found in circular orbits with low-mass He white dwarf companions. Needless to say that these expectations are in agreement with the existing body of observations on the binary pulsars.

The spin-up of a neutron star due to the matter accreted from its companion at a rate $\dot{M}_{\rm acc}$ is expected to be limited by an "equilibrium" period $P_{\rm eq}$ given (van den Heuvel 1977; Henrichs 1983) as

$$P_{\rm eq} \;=\; 2.4\, B_9^{\frac{6}{7}}\, R_6^{\frac{16}{7}}\, M_{\rm n}^{-\frac{5}{7}} \left(\frac{\dot{M}_{\rm acc}}{\dot{M}_{\rm Edd}}\right)^{-\frac{3}{7}} \quad {\rm ms} \tag{1.2}$$

where $\dot{M}_{\rm acc}$ is the rate of capture of wind matter in solar masses per year, $\dot{M}_{\rm Edd}$ is the maximum possible "Eddington limit" for the accretion rate, B_9 is the surface field strength in units of 10^9 G, and R_6 is the radius of the neutron star in units of 10^6 cm. Using $\dot{M}_{\rm Edd} = 1.5 \times 10^{-8} R_6 \;\; M_\odot \; {\rm yr}^{-1}$, and assuming $R_6 = 1$, $M_{\rm n} = 1.4 \;\; M_\odot$, and $\dot{M}_{\rm acc} = \dot{M}_{\rm Edd}$ the ***minimum*** value of $P_{\rm eq}$ is found to be

$$P_{\rm eq} \;\approx\; 2\, B_9^{\frac{6}{7}} \;\; {\rm ms} \tag{1.3}$$

which defines the so-called "spin-up" line in the pulsar B_s–P_s diagram (Radhakrishnan & Srinivasan 1984; Srinivasan & van den Heuvel 1982), as shown in Fig. 1.5 .

According to the standard picture, the evolutionary history of neutron stars in close binaries may be divided into three successive phases (Pringle & Rees 1972; Illarionov & Sunyaev 1975) as follows.

a) The (possibly obscured) radio pulsar phase, in which the radio emission from a young pulsar might be absorbed in the surrounding plasma due to the stellar wind of the companion. The pulsar's radiation pressure however keeps the accreted plasma away from the neutron star's magnetosphere.

b) The slow-down or deceleration phase, in which the magnetosphere of the neutron star acts as a "propeller", ejecting the infalling accreted wind matter.

c) The accretion or spin-up phase, in which the accreted matter falls onto the surface of the neutron star releasing its gravitational energy. A heavy mass transfer might then ensue due to the Roche-lobe overflow whence the binary starts its new life as a bright X-ray source.

A neutron star born in a close binary will therefore evolve through the following "recycling" route on the B_s–P_s diagram (see Fig. 1.5). The normal spin-down of a pulsar will first cause the spin period to increase and the star will move to the right along a horizontal track, if no magnetic field decay over the corresponding period of time occurs. This motion will finally make the pulsar to cross the "death-line" and stop functioning as a pulsar, if its companion wind has not been able to do so earlier (see § 1.4). Interaction with the stellar wind of the companion during its mainsequence phase will further increase the spin period during a 'propeller" phase until it reaches the corresponding P_{eq} for the given values of B_s and $Ed,$. The neutron star will however remain unobservable throughout this period, except for the case of those with Be-type companions which might from time to time eject some matter. This will cause a temporary increase in M_{acc} and hence a spin-up "accretion" phase making the system observable as a transient X-ray source for a few weeks. But, in general later when the companion evolves away from the mainsequence it overflows its Roche lobe (in a close binary) and the neutron star will be spun up because of the enhanced M_{acc} values which correspond to smaller P_{eq} (see Eq. 1.2). The angular momentum of the accreted matter being in Keplerian orbits around the neutron star will cause it to spin up, as is observed in the case of disk fed pulsating X-ray sources. Thus during the accretion

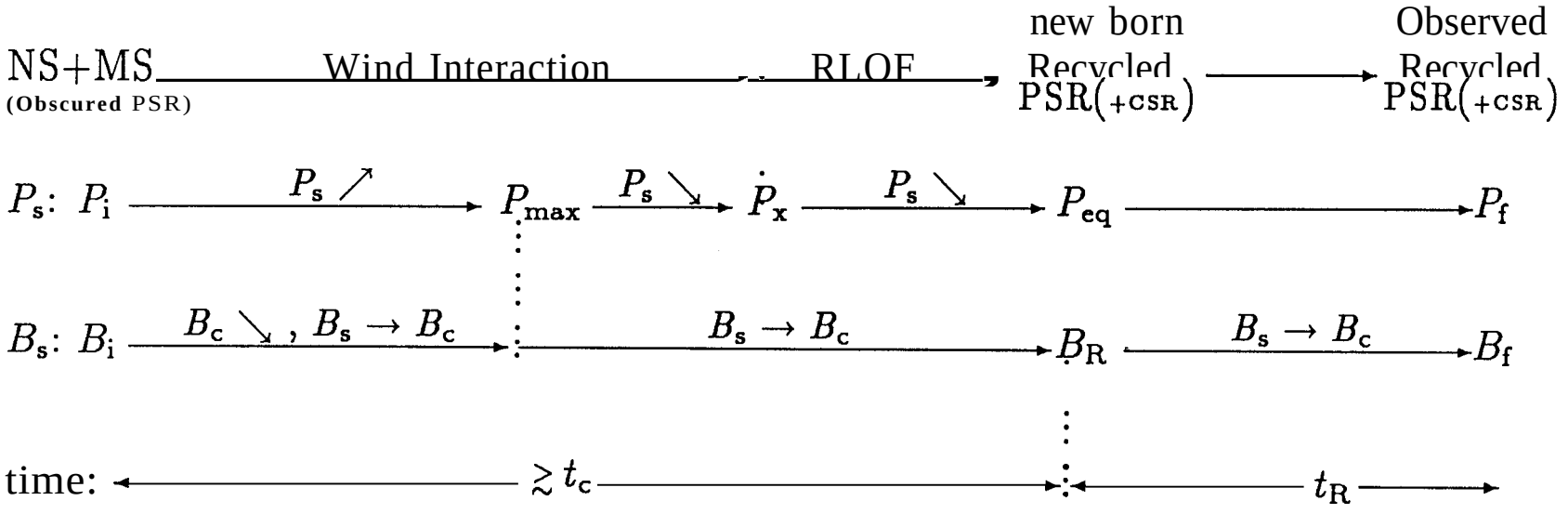

Figure 1.6- Schematic representation of the recycling scenario including the magnetic field evolution according to the model of spin-down-induced flux expulsion. The symbols are defined in the text.

phase the neutron star moves on $B_s - P_s$ diagram to the left, in addition to a vertical downward displacement which it might undergo due to the decay of its magnetic field. Since the spin-up line lies to the left of the pulsar death-line, the above motion to the left will therefore cause the neutron star to return from the graveyard and start its new recycled pulsar life somewhere on the spin-up line depending on its current surface field strength, once the mass transfer is halted.

To summarize and highlight the quantities of interest for our present study, the recycling scenario along with the implications of the spin-down induced field decay model for evolution of the surface magnetic fields B_s of neutron stars in close binary systems are shown, schematically, in Fig. 1.6. Slanted *up-* and *downward* arrows in Fig. 1.6 indicate increasing and decreasing quantities, respectively.

Fig. 1.6 depicts that a pulsar in a close binary with a mainsequence (MS) star will undergo a phase of spinning-down to a maximum period P_{max} followed by *a* phase of spinning-up both due to interaction of its magnetosphere with the matter accreted from the stellar wind of its companion. Roche-lobe overflow (RLOF) of the companion star will, at some later stage of its evolution, further decrease the spin period P_s of the neutron star (NS) bringing it from its value at the beginning of the RLOF-phase P_x to a minimum equilibrium period P_{eq}. The value of P_{eq} depends on the strength of the surface magnetic field of the neutron star at that epoch B_R and the rate of accretion of matter onto the neutron star M_{acc} **(Eq.** 1.2). In the following the Eddington accretion rate $\dot{M}_{Edd}$ will be assumed to be applicable during the RLOF-phases of all binaries of interest hence making P_{eq} a function of B_R only (Eq. 1.3). This value of P_{eq} is however only a limit on the minimum spin period which is possible through the spin-up process. The actual value achieved is further constrained by the duration and the efficiency of the RLOF-phase in each case. **A** neutron star born with an initial period P_i and field strength B_i in a close binary which would be otherwise observable as a radio pulsar is presumably being obscured in the wind of its companion **and** missed by the general radio pulsar surveys in most cases of interest (Illarionov & Sunyaev 1975; Bhattacharya & van den Heuvel 1991; Lipunov 1992). It is however expected to start

again functioning as a recycled pulsar (being either in a binary with a compact stellar remnant, CSR, or single) after a time about the MS-lifetime of its companion t_c has elapsed. The subsequent evolution of a recycled pulsar will in general cause its period and magnetic field strength to change from the starting values P_{eq} and B_R to the final observed (after a time t_R) values P_f and B_f, respectively. The evolution of the orbital period P_{orb} of the binary system is not expected to depend on the spin or magnetic evolution of the neutron star and is determined by the amount of mass transfer within the binary as well as the mass and angular momentum losses from the system.

1.3 Accretion from a Stellar Wind

A neutron star in a binary system might interact with the accreted matter which is lost by its companion due to two different processes. The companion star loses mass firstly as it emits a stellar wind during the mainsequence and the subsequent phases of its evolution. In a close binary system another possibility for mass transfer might be also realized when a star is unable to hold its surface matter against the gravitational attraction of its companion. In the latter case, viz. the so-called Roche-lobe overflow, matter is transferred through the inner Lagrangian point of the binary and forms a disk around the companion neutron star. The Roche-lobe mass transfer might occur in a binary when a star expands due to its internal nuclear evolution. Another possibility is that the Roche lobe might shrink to a size within the stellar surface as a result of a loss in the orbital angular momentum of the system (see § 1.4) which would cause the orbit to shrink.

In the studies of X-ray binary sources, accretion of the ***stellar wind*** by the neutron star has been usually invoked only in the case of ***massive*** X-ray binaries (HMXBs). The neutron star in these systems is believed to accrete from the winds of OB supergiants or Be-type companions (Henrichs 1983; Rappaport & Joss 1983). In the case of Low-mass X-ray binaries (LMXBs) however the Roche lobe overflow is considered to be the case since the wind rate of the companion is too weak to account for the observed X-ray luminosities of these sources. Nevertheless, in our study of the coupled spin-magnetic

field evolution of neutron stars accretion from the stellar wind of a mainsequence companion prior to the X-ray phase of the binary will be considered, for both massive and low-mass systems. This is because according to the adopted model the magnetic evolution of a neutron star is determined by its ***spin-down*** history. A spin-down phase is, as indicated earlier, expected to occur favorably prior to the X-ray phase in both LMXBs and HMXBs. This is partly because of the lower rates of accretion from a stellar wind of a mainsequence star as compared to its supergiant phase, or that due to the Roche lobe mass transfer. Also the larger field strengths of the younger neutron stars in the younger systems calls for a spinning down of the neutron star before the X-ray phase (see Eq. 1.2). Indeed, in our model simulations (to be discussed in chapter 2) for both low- and high-mass systems the spin-down and spin-up phases are realized successively during the mainsequence phase of the companion star. The transition from a spin-down to a spin-up phase occurs due to the adopted decay mechanism for the magnetic field of a neutron star which has been built into the simulations.

A neutron star moving in the wind of its companion star with a velocity V_{rel} is assumed to capture all the approaching matter having an impact parameter less than or equal to a maximum value of R_{acc}, the so called accretion radius. According to the Hoyle-Lyttleton scenario (Hoyle & Lyttleton 1939) wind particles follow free Keplerian trajectories until they collide with each other along the down stream accretion axis (see Fig. 1.7). The collisions are supposed to result in cancellation of the velocity components perpendicular to the axis, leaving only the parallel velocity components pointing away from the star. Accretion radius is thus determined by finding the impact parameter for which the parallel component of velocity on the axis becomes equal to the local escape velocity. Equivalently, from energy considerations it is hence found that

$$R_{a} = \frac{2G M_{n}}{V_{rel}^{2}} \tag{1.4}$$

where M_n is the mars of the neutron star, and $V_{rel} = (V_w^2 + V_{orb}^2)^{1/2}$ where V_{orb} is the orbital velocity of the neutron star, and V_w is the velocity of the wind with respect to the mass-losing star (see Fig. 1.7). The accretion rate M_{acc} is determined by calculating

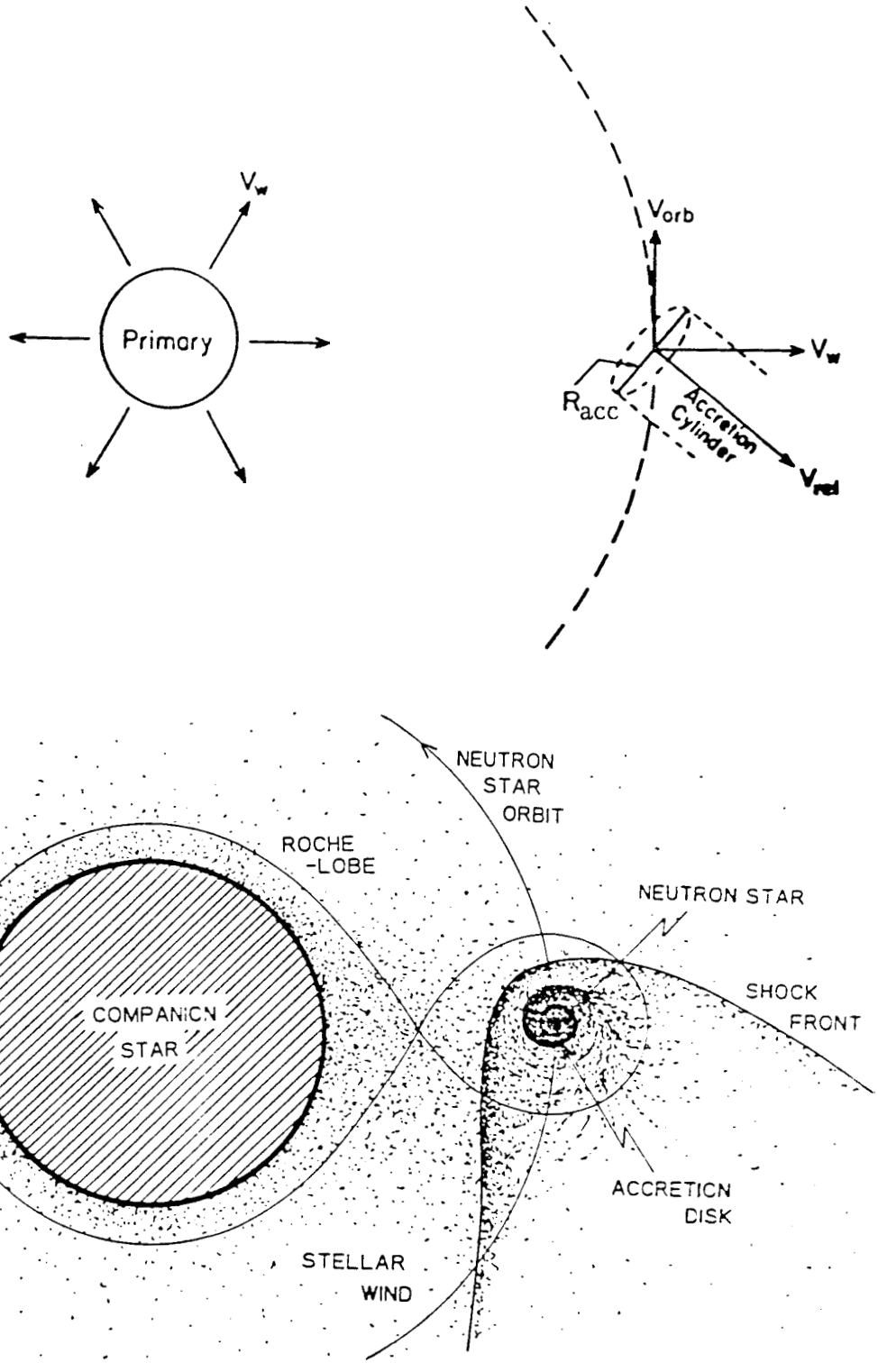

Figure **1.7**- Accretion by a compact object (say a neutron star) from the stellar wind of its binary companion. The relative directions of accretion cylinder and different velocities are shown at the *top.* An accretion disk might form near the neutron star and behind ihe shock front in the converging wind as shown in the *bottom.* [from Nagase 1989]

the rate of matter flowing through the accretion cylinder, which is the cylinder of radius $R_{\rm acc}$ with its axis passing through the neutron star and parallel to the upstream particles velocity. Thus

$$\dot{M}_{\rm acc} = \pi R_{\rm acc}^2 \rho_\infty V_{\rm rel} \tag{1.5}$$

For the above Hoyle-Lyttleton approximation therefore the accretion rate may be given

$$\dot{M}_{\rm HL} = \equiv \frac{4\pi G^2 \rho_\infty M_{\rm n}^2}{V_{\rm rel}^3} \tag{1.6}$$

where ρ_∞ is the density of the wind matter just before being deflected onto the neutron star, ie. at a large distance upstream. The density of the stellar wind at any distance r' from the mass losing star can be found from the continuity equation for the flow, namely

$$|\dot{M}_2| = 4\pi r'^2 \rho(r') V_{\rm rel}(r') \tag{1.7}$$

where $\dot{M}_2$ is the rate of the mass-loss from the companion star in the form of a spherically symmetric stellar wind.

The accretion axis invoked above being a geometrical line however implies a singularity in the density of the converging matter. An improvement due to considering instead a more physical, finite density, accretion cone has led (Bondi & Hoyle 1944) to the accretion rate

$$\dot{M}_{\rm BH} = \alpha_{\rm acc} \dot{M}_{\rm HL} \tag{1.8}$$

where $1/2 \leq \alpha_{\rm acc} < 1$ is an unknown parameter which depends on the initial conditions. The above derivations of the accretion rate however neglect the effects due to the gas pressure, since they were based on the dynamics of single particles trajectories which is a valid approximation only for highly supersonic flows. The hydrodynamical treatment of the problem has nevertheless resulted in the following general formula for the accretion rate (Davidson & Ostriker 1973; Alcock & Illarionov 1980; Ghosh & Lamb 1991)

$$\dot{M}_{\rm acc} = \frac{4\pi G^2 \rho_\infty M_{\rm n}^2}{(V_{\rm rel}^2 + C_\infty^2)^{\frac{3}{2}}} \tag{1.9}$$

where C_∞ is the sound velocity in the wind upstream.

Using Eqs 1.4, 1.5, 1.7, and 1.9 and assuming $\rho_\infty = \rho(r' = a)$, the radius and the rate of accretion will be calculated in our simulations from

$$R_{\rm acc} = 3.83 \times 10^5 \left(\frac{M_{\rm n}}{V_{\rm rel}^2 + C_{\rm s}^2}\right) R_\odot \tag{1.10}$$

$$\dot{M}_{\rm acc} = \left(\frac{R_{\rm acc}}{2a}\right)^2 \left(\frac{V_{\rm rel}}{V_{\rm w}}\right) |\dot{M}_2| \tag{1.11}$$

where all the velocities are in units of km/s, and $M_{\rm n}$ is in solar unit.

1.4 Spin Evolution

A homogeneous wind (in density and velocity) entering into the accretion cylinder would have zero net angular momentum with respect to the neutron star. Indeed the basic underlying assumption in the above Hoyle-Lyttleton picture is the exact cancellation of the transverse velocities of the wind particles, which will make the subsequent infall along the down-stream accretion axis possible. The spin period of a neutron star accreting from such an idealized homogeneous wind would not be therefore changed due to its interaction with the accreted matter. The density of the matter in a stellar wind is however expected to decrease with increasing distance from the star, as required by the continuity equation (Eq. 1.7). The wind velocity might be constant or the wind might be speeding up as is believed to be the case in particular for the massive stars where radiation pressure due to resonant scattering of the stellar uv-photons by ions in the wind is believed to accelerate the wind (eg. Lucy & Solomon 1970). During the outflow from the stellar surface the wind is accelerated to a typical terminal velocity of a few times the escape velocity at the stellar surface. The wind velocity $V_{\rm w}$ as a function of the distance r' from the star is given (eg. Abbott 1978) as

$$V_{\rm w} = k(r') \sqrt{\frac{2G\,M}{R}} \tag{1.12}$$

where k $\sim$ 3 is attained at r' of a few times the stellar radius R. We will be however considering a constant wind velocity for any star of a given mass assuming that for the binaries which are considered here the wind velocity close to the neutron star has already achieved its terminal velocity. Matter entering the accretion cylinder would be therefore denser at those points of the cylinder cross section which are closer to the companion star (see Fig. 1.7).

The specific angular momentum l of the accreted matter could be in general calculated by approximating the variations in the density and the velocity with their first order expansions about the center of the cylinder. This result in

$$l = \frac{\eta}{2} \Omega_{\rm orb} R_{\rm acc}^2 \qquad (1.13)$$

where $\Omega_{\rm orb} = \frac{2\pi}{P_{\rm orb}}$, and η is a numerical parameter of order unity which depends on the variation of the density and velocity of the wind across the capture area. The maximum possible angular momentum carried by the wind is thus found to be comparable with that in the case of disk accretion (Nagase 1989). It is not however clear how much of this is actually deposited onto the neutron star when it is finally accreted. While some authors have assumed that all of the above angular momentum (Eq. 1.13) is transferred to the accreting neutron star (Illarionov & Sunyaev 1975; Wang 1981) others have argued that in this case too, as for a homogeneous wind, no angular momentum is accreted at all (Davies & Pringle 1980). Nevertheless, the earlier 2D and the more recently emerging 3D numerical hydrodynamical simulations seem to have established that angular momentum is indeed accreted from a nonhomogeneous wind, even though possibly at a rate somewhat smaller than that given by Eq. 1.13 (Livio 1994). In some of these calculations even a disk is also seen to form around the accreting center, which in some cases exhibits reversal of its sense of rotation quasi periodically (Taam & Fryxell 1988; Fryxell & Taam 1988). A disk is believed to be formed around an accreting object if the specific angular momentum of the converging matter is larger than that of the closest possible circular Keplerian orbit which will form the inner edge of the disk. In the case of a neutron star the inner radius of the disk has to be larger than the radius of the star's magnetosphere $R_{\rm mag}$ (see below). The specific angular

momentum of the accreting matter therefore has to be larger than that of a circular Keplerian orbit of the radius $R_{\rm mag}$, for a disk to be formed around a neutron star. Thus, the observed formation of a disk in the 3D simulations indicates a minimum limit for the angular momentum of the matter accreted from a stellar wind in a binary system.

1.4.1 The Magnetosphere

Accretion of the matter captured by the gravitational attraction of a neutron star, whether forming a disk or as a spherical infall, is on the other hand impeded by the electromagnetic field of the star. The energy radiated by a rotating magnetized neutron star in the form of relativistic particles and/or electromagnetic radiation is assumed to originate somewhere at a characteristic distance of the so-called light cylinder radius $R_{\rm l}$ defined as

$$R_{\rm l} = \frac{c}{\Omega} \equiv \frac{cP_{\rm s}}{2\pi} \tag{1.14}$$

where Ω is the angular rotation frequency of the neutron star.

At distances from the neutron star $r < R_{\rm l}$ the electromagnetic field is static and since the wind matter is expected to be a highly conductive plasma it cannot penetrate through the field. The wind will instead act like a dimagnetic and will try to squeeze the field. By balancing the pressure $P_{\rm mag}$ of the assumed dipolar magnetic field around the star with the ram pressure $P_{\rm gas}$ of the matter, the radius $R_{\rm mag}$ of the magnetosphere might be therefore determined. We use

$$P_{\rm mag}(r) = \frac{B^2(r)}{8\pi} = \frac{B_{\rm s}^2 R_{\rm s}^6}{8\pi r^6} \tag{1.15}$$

$$P_{\rm gas}(r) = \rho(r)\, v^2(r) \tag{1.16}$$

where $\rho(r)$ is the density and $v(r)$ is the velocity of the matter at a distance r from the neutron star, and $R_{\rm s}$ is the radius of the neutron star. The matter after entering the accretion cylinder would be freely falling onto the neutron star. In this regime

the velocity $v(r)$ and the density $\rho(r)$ of the accreting gas obey the following general relations, for the case of spherical accretion,

$$v(r) = \sqrt{\frac{2GM_{\rm n}}{r}} \tag{1.17}$$

$$\rho(r) = \frac{\dot{M}_{\rm acc}}{4\pi r^2\, v(r)} \tag{1.18}$$

Substituting for v and p from Eqs 1.17, and 1.18 into Eqs 1.15, and 1.16 and using the pressure balance relation, ie.

$$P_{\rm mag}(r = R_{\rm mag}) = P_{\rm gas}(r = R_{\rm mag}) \tag{1.19}$$

$R_{\rm mag}$ is derived as

$$R_{\rm mag} = (2GM_{\rm n})^{-\frac{1}{7}}\,(B_{\rm s}R_{\rm s}^3)^{\frac{4}{7}}\,\dot{M}_{\rm acc}^{-\frac{2}{7}} \tag{1.20}$$

It is noted that the value of $R_{\rm mag}$ for the case of disk accretion is also expected to be similar to the above value, although both smaller and larger values than the above estimate have been derived by different authors depending on the different values which they have assumed for the radial velocity of the matter in both cases of disk and spherical accretion (Nagase 1989; Wang 1981). At distances $r \leq R_{\rm mag}$ the magnetic field is so strong that it will determine the motion of the matter which is hence forced to co-rotate with the neutron star.

The expression for $R_{\rm mag}$ in Eq. 1.20 is not however valid if the conditions are such that $P_{\rm mag} > P_{\rm gas}$ at $r = R_{\rm acc}$ which implies that the radius of the magnetosphere is larger than $R_{\rm acc}$. Note that in this case the condition $P_{\rm mag} > P_{\rm gas}$ will persist throughout the region inside the accretion cylinder since $P_{\rm mag}$ *or* r^{-6} and $P_{\rm gas}$ *or* $r^{-\frac{5}{2}}$. Outside the accretion cylinder, which is also assumed to be bounded by a shock front at a distance of $\sim R_{\rm acc}$ up-stream from the neutron star (see Fig. 1.7), the motion of the gas is unaffected by the gravitation of the neutron star. Hence Eqs 1.17 and 1.18 which assume the gas is falling under the effect of the gravitation of the neutron star are not valid. Given the velocity law for the outflow of the stellar wind from the mass-losing star then $V_{\rm w}(r)$ is known and the density of the gas in this case may be however determined from the continuity equation, namely

$$\rho(r) \;=\; \frac{|\dot{M}_2|}{4\pi(a - R_{\rm mag-out})^2\, V_{\rm w}(r)} \tag{1.21}$$

The magnetospheric radius for the case when it is located outside the accretion cylinder $R_{\rm mag-out}$ might therefore be estimated still from the pressure balance equation (Eq. 1.19) which reduces to

$$\left(\frac{2\dot{M}_2}{B_{\rm s}^2 R_{\rm s}^6}\frac{V_{\rm rel}^2}{V_{\rm w}}\right)^{\frac{1}{2}} R_{\rm mag-out}^3 + R_{\rm mag-out} - a \;=\; 0 \tag{1.22}$$

It has to be recalled that the magnetosphere of a neutron star is bounded by the light cylinder of the radius $R_{\rm l}$ (Eq. 1.14). If the calculated value of $R_{\rm mag}$ from Eq. 1.20 (or $R_{\rm mag-out}$ from Eq. 1.22) turns out to be larger than $R_{\rm l}$ then it is set equal to $R_{\rm l}$.

Furthermore, the accretion rate $\dot{M}_{\rm acc-in}$ for the case when magnetosphere extends beyond the accretion cylinder also cannot be calculated by use of the general definition of the accretion radius (Eqs 1.4 and 1.5), which has been adopted by some authors (Liuponov 1992) for this case too. This is because the accretion radius is determined from a balance of the gravitational and kinetic energies of the freely moving matter. In the present case however the matter encounters the magnetosphere before getting close enough to the neutron star to feel its gravitation and its kinematics is different than outside the magnetosphere. In the absence of any theoretical treatment of the problem of accretion by a neutron star for such a case, we use the suggested rate given in analogy with the accretion rate of the solar wind by the Earth's magnetosphere (Alcock & Illarionov 1980). The accretion rate in the case of geomagnetosphere, which is also situated outside the corresponding accretion radius as defined by Eq. 1.4, is estimated to be $\sim \frac{1}{1000}$ of that due to the geometrical cross section of the magnetosphere, which results in

$$\dot{M}_{\rm acc-in} \;=\; \frac{|\dot{M}_2|}{1000}\frac{V_{\rm rel}}{V_{\rm w}}\frac{R_{\rm mag-out}^2}{4\,(a - R_{\rm mag-out})^2} \tag{1.23}$$

1.4.2 Radiation-pressure Dominated Regime

For the accreting wind matter within the accretion cylinder in order to reach the magnetosphere and be able to interact with the neutron star it has to first overcome the obstacle due to the pressure of the relativistic particles as well as the electromagnetic radiation (the pulsar wind) emitted by the star, in the region $r > R_l$. The energetic particles in the pulsar wind are expected to be "trapped" in the magnetic field of an accreting plasma and hence impart momentum to it, ie. present pressure against the incoming plasma. This is because for the typical random magnetic fields in the stellar wind the Larmor radius of the energetic particles is found to be much smaller than the accretion radius (Liuponov 1992). Also the associated plasma frequency of the accreting wind matter is larger than the frequency of the magnetic dipole radiation and hence the radiation is reflected by the wind matter. The total pressure P_{rad} due to the particles and radiation field emitted by a neutron star at a distance r from the star is estimated as

$$P_{rad} = \frac{L_{PSR}}{4\pi r^2 c} \qquad (1.24)$$

where L_{PSR} is the total rate of energy loss by the neutron star and is given, in analogy with the case of purely magnetic dipole radiation, as

$$L_{PSR} = \frac{2}{3c^3} B_s^2 R_s^6 \left(\frac{2\pi}{P_s}\right)^4 \qquad (1.25)$$

The balance between the radiation and the gas pressure will determine the distance R_{rad} from the neutron star at which the matter infall towards the star might be brought to a halt by the pulsar wind. It is noted that depending on whether $R_{rad} < R_{acc}$ or $R_{rad} > R_{acc}$ the P_{gas} and $\dot{M}_{acc}$ have to be calculated self-consistently from the appropriate relations, as discussed earlier for the calculation of R_{mag} (see discussions related to Eqs *1.22* and ***1.23).***

An explicit evaluation of R_{rad} is not however required in either cases and one needs only to compare values of P_{rad} and P_{gas} at $r = R_l$ in order to determine the expected phase of the pulsar spin evolution. If $R_{rad} > R_l$ (viz. $P_{rad} > P_{gas}$ at $r = R_l$) *a* cavern is formed around the neutron star (see Fig. 1.8) and no dynamical coupling between

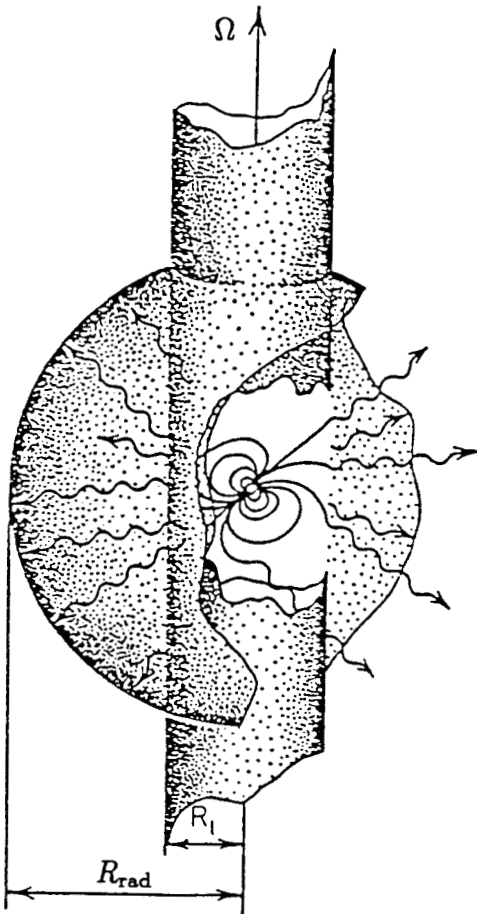

Figure 1.8- Schematic representation of the light cylinder with a radius R_l and the radiation field around a rotating magnetized neutron star in the ***Active** pulsar **phase.*** The balance between radiation pressure, mainly due to the outflowing relativistic particles and/or magnetic dipole radiation, and gas pressure of the matter attracted by the gravitation of the star is achieved at a distance of R_{rad}. [adopted from Lipunov 1992]

the star and the accretion matter can occur. The star will be therefore slowing down in this phase, namely the (possibly obscured) active radio pulsar phase, due only to its intrinsic decelerating torque. The spin-down rate of the neutron star P_s in this phase may be derived from

$$L_{\rm PSR} \equiv I\,\Omega\,\dot{\Omega} \tag{1.26}$$

where $\dot{\Omega}$ is the rate of change of the spin frequency R, and which results in

$$\dot{P}_s = 10^{-23}\,\frac{B_8^2}{P_s}\ \ {\rm ss}^{-1} \tag{1.27}$$

where B_8 is the surface field strength in units of 10^8 G.

1.4.3 Gas-pressure Dominated Regime

However, when the pulsar radiation pressure is not strong enough to stop the infalling accreted matter, i.e. $R_{\rm rad} < R_{\rm l}$, the accreted matter makes contact with the magnetosphere and may cause a spin-down or spin-up of the star. Namely the matter once it reaches the magnetosphere might extract extra angular momentum from it and be be thrown off or else it would settle onto the neutron star adding to star's specific angular momentum. For the case of disk accretion the rate of the transfer of angular momentum between the neutron star and the matter rotating in Keplerian orbits around the star due only to mechanical stresses is estimated (Illarianov & Sunyaev 1975) as

$$\dot{L}_s = \dot{M}_{\rm acc}\,R_{\rm mag}\,V_{\rm dif}(r = R_{\rm mag}) \tag{1.28}$$

where $V_{\rm dif}(r = R_{\rm mag}) = V_{\rm corot} - V_{\rm Kep}$ is the difference between the co-rotation velocity $V_{\rm corot}(r)$ with the magnetosphere and the Keplerian velocity $V_{\rm Kep}(r)$ both evaluated at a distance $r = R_{\rm mag}$. The rate of angular momentum transfer for the spin-up and the spin-down phases may be therefore calculated in both cases from Eq. 1.28 depending on the sign of $V_{\rm dif}$. The change in the sign of the quantity $V_{\rm dif}$ may be determined also from a comparison between the values of the so-called co-rotation radius $R_{\rm co}$ and $R_{\rm mag}$. The plasma entering the magnetosphere is frozen in the magnetic field and is

dragged along with it to co-rotate with the star. There exists however a surface S_{co} (see Figs 1.9 and 1.10) beyond which the velocity of particles (when forced to co-rotate with the magnetosphere) is too high to let them fall toward the star. The co-rotation surface is defined by the balance between the gravitation and the centrifugal forces on an assumed co-rotating particle. Namely at a radial distance r from the center of the star and at an angle θ away from the equator the relation

$$r\,\Omega\,\cos\theta \;=\; \sqrt{\frac{GM_n}{r}} \tag{1.29}$$

must be satisfied for particles on S_{co}. The equation for the generator of the co-rotation surface is thus given (Liuponov 1992) as

$$r \;=\; R_{co}\,\cos\theta^{-\frac{2}{3}} \tag{1.30}$$

where $R_{co} = \left(\frac{GM_n}{\Omega^2}\right)^{\frac{1}{3}}$ is the co-rotation radius at the equator. The positive or negative sign of V_{dif} which corresponds to the conditions for the propeller or the accretion phase, respectively, could be therefore expressed also as $R_{co} < R_{mag}$ (Fig. 1.9) and $R_{co} > R_{mag}$ (Fig. 1.10), respectively.

Nevertheless, due to the additional magnetic coupling of the infalling matter with the magnetosphere the interaction between them might however occur simultaneously over an extended boundary region. This is in contrast to the unique distance of R_{mag} which was assumed for the case of mechanical coupling that leads to Eq. 1.28 for the transmitted torque. The magnetic coupling has been studied in detail for the case when the stellar magnetic axis is aligned with the disk axis (Ghosh, Lamb & Pethick 1977, Ghosh & Lamb 1991). The results of these studies however show that for the limiting cases of very slow and very fast rotations of the neutron star the torque is similar to that due to the mechanical stresses exerted at R_{mag} (Nagase 1989), namely that given by Eq. 1.28. In addition, our rough estimate of the accretion torque (Eq. 1.28) might be excused particularly for the discussions in chapter 2 because the important quantity relevant to the adopted field decay model is the *maximum* ***spin period*** which a neutron star acquires during its lifetime. The improvement in the results due to any other detailed treatment of the torque history would be only in possible changes in the time

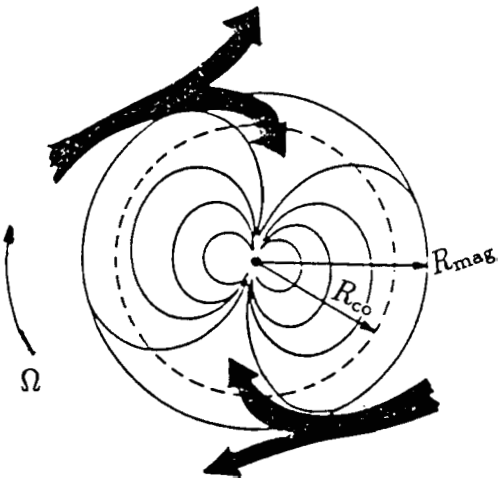

Propeller

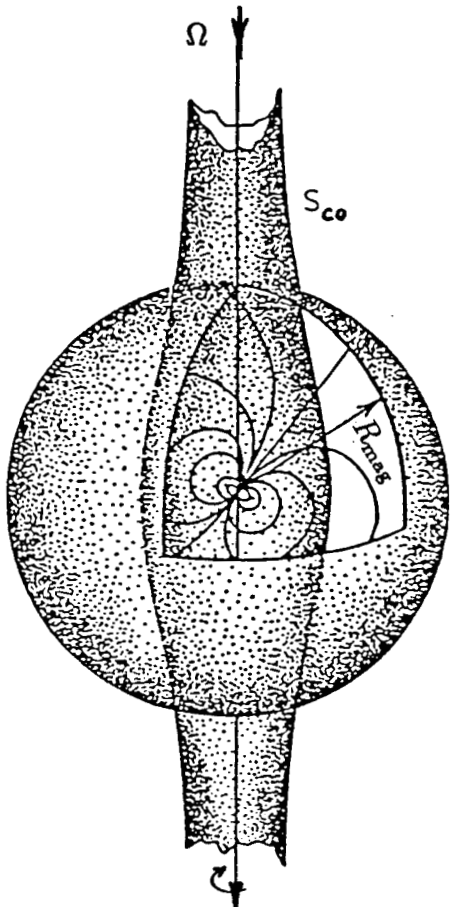

Figure 1.9- As Fig. 1.8 but for the case of a *Propeller phase.* When $R_{mag} = R_{co}$ the neutron star spins at its equilibrium spin period P_{eq} which is expected not to be changed by further accretion. [adopted from Schreier 1977, and Lipunov 1992]

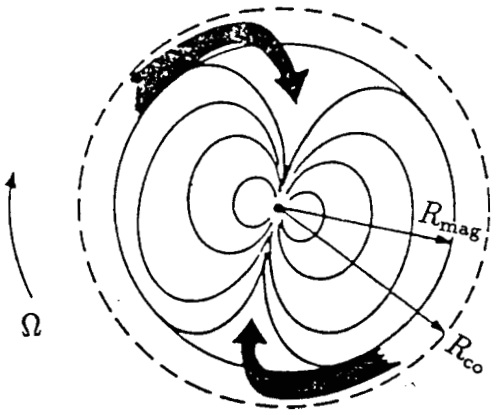

Accretion

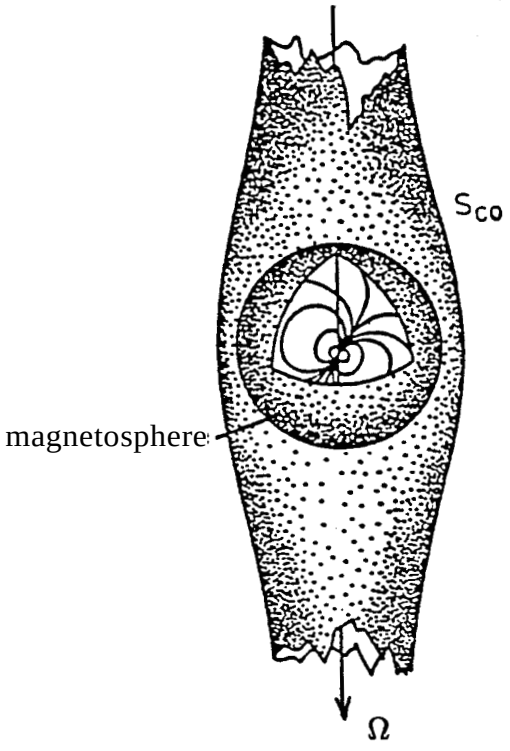

Figure1.10- Schematic representation of the magnetosphere at a radius R_{mag} and the co-rotation surface S_{co} with an equatorial radius R_{co} for a rotating magnetized neutron star in the *Accretion phase,* as viewed along *(top)* and away from *(bottom)* the rotation axis. [adopted from Schreier 1977, and Lipunov 1992]

scale and the exact spin history of the star in arriving at a final value of P_{eq} (along the spin-up line) which is decided only by the field strength B_s and the accretion rate M_{acc}. As long as the difference in the time scales of the spin-down phase due to the different plausible evaluations of the torque is not larger than the assumed decay time scale of the field in the crust of neutron stars the predicted field evolution would be essentially the same. Also it is noted that the torque given by Eq. 1.28 for the case of a spin-up phase is less than that expected even for the mechanical coupling at R_{mag}; namely V_{dif} has to be replaced with V_{Kep}. The spin-up of the neutron star has no effect on the further evolution of its magnetic field in our calculations and the above relation for angular momentum transfer has been used to ensure the occurrence of an equilibrium spin period, without resorting to a detailed and complicated modeling (as in, say, Ghosh et. al. 1977). However in order to test the results of other estimates of $\dot{L}_s$ different than that in Eq. 1.28 it might be modified to the following form

$$\dot{L}_s = \xi \dot{M}_{acc} R_{mag} V_{dif} \tag{1.31}$$

where we have introduced an efficiency factor ξ for which different values will be used in our simulations of binary evolution of neutron stars, and $\xi = 1$ reproduces Eq. 1.28.

The rate of change of the spin period of the star due to the accretion torque $\dot{L}_s$ would furthermore depend also on the sense and the angle of the rotation axis of the neutron star with respect to the orbital plane, the latter being same as the plane of the accretion disk. Here we will consider only the case where the stellar axis and the disk axis are parallel, and also assume that the matter in the disk is rotating in the same sense as the neutron star. These assumptions might be justified as representing the most probable cases since they correspond to the presumably aligned and synchronous rotation of the neutron star's progenitor in the binary.

The spin evolution of a neutron star during the propeller and the *accretion* phases can be thus calculated using the dynamical equation

$$\dot{L}_s = I \dot{\Omega} \equiv \frac{-2\pi I \dot{P}_s}{P_s^2} \tag{1.32}$$

where I is the total moment of inertia of the neutron star. Substituting for $\dot{L}_s$ from

Eq. 1.31 the rate $\dot{P}_s$ of change of the spin period of the neutron star due to interaction with accreted matter is derived as

$$\begin{aligned} \dot{P}_s &= \frac{\dot{M}_{acc}\, R_{mag}\, P_s^2}{2\pi I}\, \xi\, V_{dif} \\ &= 10^{-24}\, \xi\, \dot{M}_{-14}\, R_{mag}\, V_{dif}\, P_s^2 \quad ss^{-1} \end{aligned} \tag{1.33}$$

where R_{mag}, V_{dif}, and P_s are in units of km, km s^{-1}, and s, respectively. Note that the sign of $\dot{P}_s$ is decided by that of V_{dif}.

1.5 Orbital Evolution

The orbital separation a of the binary clearly affects the estimated value of $\dot{P}_s$ given by Eq. 1.33, and its time behavior ought to be determined. The orbital evolution of a binary system under mass exchange between the components and/or mass loss from the system may be determined from the expression for the total orbital angular momentum L_{orb}; namely

$$L_{orb} = M_1 M_2 \sqrt{\frac{Ga}{M}} \tag{1.34}$$

where M_1 and M_2 are the masses of the two stars, M = $M_1 + M_2$. Differentiating with respect to the time results in

$$\frac{a}{a} = 2\frac{\dot{L}_{orb}}{L_{orb}} - 2\frac{\dot{M}_1}{M_1} - 2\frac{\dot{M}_2}{M_2} + \frac{\dot{M}}{M} \tag{1.35}$$

where a dot indicates the time derivative of the corresponding quantity. The rate $\dot{L}_{orb}$ of change of the orbital angular momentum may be expressed as

$$L_{orb} = L_{esc} + L_{losses} \tag{1.36}$$

where L_{esc} denotes the change in L_{orb} due only to the matter escaped from the binary system, and $\dot{L}_{losses}$ is that due to the other causes (see below). Let M_2 be the mass of the mass-losing star, then if a fraction α of the matter which is lost by the mass losing star leaves the system (and the rest falls on its companion) the rate of total mass-loss M from the binary system may be written as

$$\dot{M} = \alpha\, \dot{M}_2 \tag{1.37}$$

where both $\dot{M}_2$ and $M < 0$, and $0 \leq a \leq 1$. Similarly, the specific angular momentum L_{esc}/M carried away by the matter leaving the binary is defined in terms of that of the matter in the mass losing star as

$$\frac{\dot{L}_{esc}}{\dot{M}} = \beta \frac{L_2}{M_2} \tag{1.38}$$

where L_2 is the orbital angular momentum of the star with mass M_2. Substituting for M and L_2 in Eq. 1.38 then results in

$$\frac{L_{esc}}{L_{orb}} = \alpha \beta \frac{\dot{M}_2}{M_2} \frac{M_1}{M} \tag{1.39}$$

Using Eqs 1.36, 1.37, and 1.39 Eq. 1.35 may be rewritten in the following form

$$\frac{a}{a} = -2\left[1 - (1-\alpha)\frac{M_2}{M_1} - \frac{\alpha}{2}\frac{M_2}{M} - \alpha\beta\frac{M_1}{M}\right]\frac{\dot{M}_2}{M_2} + 2\frac{\dot{L}_{losses}}{L_{orb}} \tag{1.40}$$

where α and β define the mass lost from the binary and its associated loss of orbital angular momentum as defined (Eqs 1.37 and 1.38). This is the equation which we use for a determination of orbital evolution in our model computations. It remains to give the prescription for calculating the values of α, β, and $\dot{L}_{losses}$ which is dealt with in the following remaining pages of this chapter.

The matter converging on the neutron star (at the rate $\dot{M}_{acc}$; cf. § 1.3) might however fail to actually accrete onto the star. Conditions at the boundary region of the magnetosphere, or even before that in the radiation zone of the pulsar, might be such that part or all of the matter captured from the wind is further lost from the gravitation pull of the neutron star and the binary system (cf. § 1.4). In the steady state it will be assumed that all of the matter entering the accretion cylinder is either accreted completely or else leaves the binary system. Thus,

$$\dot{M}_1 = \begin{cases} \dot{M}_{acc} & \ldots \quad \ldots \quad \text{accretion phase} \\ 0 & \ldots \quad \ldots \quad \ldots \quad \text{otherwise} \end{cases} \tag{1.41}$$

is used, and the factor α is determined from

$$\alpha = 1 + \frac{\dot{M}_1}{\dot{M}_2} \tag{1.42}$$

For a determination of β two separate contributions have to be considered. One is due to the matter lost by the binary system directly from the companion star and the other is that due to the matter which is first captured by the neutron star gravitation and then is either lost from the system or accretes onto the neutron star. The part of the wind which leaves the system without interacting with the neutron star carries away a specific angular momentum equal to that of the mass losing star. Therefore $\beta = 1$ for a fraction $(1 - \frac{\dot{M}_{\rm acc}}{\dot{M}})$ of the matter lost from the binary. For the rest of the matter, if it is accreting the associated loss of orbital angular momentumis equal to the gain of spin angular momentum by the neutron star. The effective value of β, taking into account also the contribution due to the matter lost directly, is thus calculated in this case as

$$\begin{aligned} \beta &= 1 + \frac{1-a}{a} \frac{R_{\rm mag}\, M^{\frac{3}{2}}\, |V_{\rm dif}|}{G^{\frac{1}{2}}\, a^{\frac{1}{2}}\, M_2{}^2} \quad \ldots \quad \ldots \text{ accretion phase} \\ &\equiv 1 + 2.29 \times 10^{-3} \left(\frac{1-\alpha}{\alpha}\, a^{-\frac{1}{2}}\, R_{\rm mag}\, M_2^{-2}\, M^{\frac{3}{2}}\, |V_{\rm dif}| \right) \end{aligned} \tag{1.43}$$

where length scales and masses are in solar units and $|V_{\rm dif}|$ is in units of km $\rm s^{-1}$. Alternatively, for the case when the matter is expelled upon interaction with the magnetosphere it will be assumed that it leaves the system with its corresponding Keplerian velocity around the neutron star at the magnetosphere boundary. The specific angular momentum carried away would be hence that of the orbital motion of the neutron star plus that of the Keplerian velocity of the matter around the neutron star. This together with the contribution from the matter lost directly then gives

$$\beta = \alpha + (1-\alpha) \left[\left(\frac{M_1}{M_2} \right)^2 + \left(\frac{R_{\rm mag}}{a} \right)^{\frac{1}{2}} \left(\frac{M}{M_2} \right)^{\frac{3}{2}} \right] \quad \ldots \text{ propeller phase} \tag{1.44}$$

which is derived for the propeller phase, but will be also used for the comparatively short period of the active pulsar phase too.

Finally, for the last term in Eq. 1.40, ie. $L_{\rm losses}$, the effects due to two other sinks of the orbital angular momentum namely magnetic braking and gravitational waves are taken into account, hence

$$\dot{L}_{\rm losses} = \dot{L}_{\rm MB} + \dot{L}_{\rm GR} \tag{1.45}$$

where the two terms on the right hand side are defined as follows.

- The spin rotation of a mass losing star is believed to be continuously slowed down since the stellar wind is forced to co-rotate with the star out to large distances because of the effect of the stellar magnetic filed on the highly conducting ionized wind matter. The requirement for a synchronous rotation of normal stars, at a rate same as the orbital frequency, in close binary systems then results in the spin angular momentum to be compensated from the orbit. The rate of loss of spin (or equivalently orbital) angular momentum due to this magnetic braking mechanism is given (Verbunt & Zwaan 1981) as

$$\dot{L}_{\rm MB} = -0.5 \times 10^{28} f^{-2} k^2 R_2^4 M_2 \left(\frac{2\pi}{P_2}\right)^3 \quad {\rm g\,cm^2\,s^{-1}} \qquad (1.46)$$

where R_2 is the radius of the star, k is a structure dependent constant defined through $\mathrm{I} = k^2 M_2 R_2^2$ where I is the moment of inertia of the star, the constant f depends on the evolutionary stage of the star and is a measure of the strength of the magnetic field of the star, and P_2 is the spin period of the star which in our case will be equal to the orbital period of the binary. Thus the relative rate of loss of orbital angular momentum due to the magnetic braking is found, using Eq. 1.31, as

$$\frac{\dot{L}_{\rm MB}}{L_{\rm orb}} = -9.58 \times 10^{-14} f^{-2} k^2 a^{-5} R_2^4 M_1^{-1} M^2 \quad {\rm s^{-1}} \qquad (1.47)$$

where masses and length scales are in solar units.

- For the gravitational radiation due to the orbital motion of the stars, the loss of orbital angular momentum is given (Shapiro & Teukolsky 1983) as

$$\dot{L}_{\rm GR} = \frac{-32 G^{\frac{7}{2}}}{5c^5} \frac{M_1^2 M_2^2 M^{\frac{1}{2}}}{a^{\frac{7}{2}}} \qquad (1.48)$$

which results in

$$\frac{L_{\rm GR}}{L_{\rm orb}} = -\frac{32 {\rm G}^3}{5c^5} \frac{M_1 M_2 {\rm M}}{{\rm a}^4}$$
$$= -2.66 \times 10^{-17} a^{-4} M_1 M_2 M \quad {\rm s^{-1}} \qquad (1.49)$$

where all the masses and a are in solar units.